Nanocrystalline magnetic alloys and ceramics

M PAL and D CHAKRAVORTY

Indian Association for the Cultivation of Science, Jadavpur, Kolkata 700 032, India
e-mail:mlsdc@mahendra.iacs.ernet.in

Abstract. Magnetic properties of materials in their nanocrystalline state have assumed significance in recent years because of their potential applications. A number of techniques have been used to prepare nanocrystalline magnetic phases. Melt spinning, high energy ball milling, sputtering, glass-ceramization and molecular beam epitaxy are some of the physical methods used so far. Among the chemical methods, sol–gel and co-precipitation routes have been found to be convenient. Ultrafine particles of both ferro- and ferri-magnetic systems show superparamagnetic behaviour at room temperature. Coercivity (H_c) and maximum energy product (BH)$_{max}$ of the magnetic particles can be changed by controlling their sizes. The present paper reviews all these aspects in the case of nanocrystalline magnetic systems – both metallic and ceramics.

Keywords. Nanocrystalline; magnetic phases; magnetic alloys.

1. Introduction

Magnetic properties of nanometer-sized particles of both ferrimagnetic and ferromagnetic materials have attracted considerable attention in recent years (Kodama *et al* 1996; Mantinez *et al* 1998; Zhang *et al* 1998). Such interest has been generated for practical as well as theoretical reasons. Some of the application areas being explored are in high-density magnetic recording media (Parker *et al* 1996), as ferrofluids (Dormann & Fiorani 1992), giant magnetoresistive systems as sensors (Parkin *et al* 1990). Some of the properties exhibited by magnetic nanoparticles that have led to basic investigations are superparamagnetism (Kittel 1946), quantum tunneling of magnetization (Chudnovsky & Gunther 1988), enhanced coercivity (Knella & Luborsky 1963), effect of exchange anisotropy in magnetic core-shell structures where the core and the shell comprise of a ferromagnetic metal and antiferromagnetic oxide respectively (Prados *et al* 1999).

A number of techniques both physical and chemical have been developed to prepare nanosized magnetic particles. In this paper, the various methods used till date to synthesize nanoparticles of ferromagnetic and ferrimagnetic systems and their magnetization characteristics are reviewed.

2. Experimental methods

2.1 *Physical methods*

2.1a *Melt spinning:*   This technique is very useful for the preparation of two-phase materials in which a hard magnetic phase is coupled to a soft one. Starting materials consist of three to five elements which on heating in some inert atmosphere (generally by arc-melting) give an alloy ingot. These ingots are then crushed into small pieces for melt spinning. Quartz crucibles with a nozzle diameter less than one mm are used for this purpose. Melt spun amorphous ribbon samples with various thicknesses are prepared by using single roll melt spinning equipment with a copper roll in an inert atmosphere. The amorphous samples have to be sealed in an evacuated quartz tube and annealed for various period (Ping & Hono 1998). This technique has a minimal interface contamination and can produce almost porosity free samples. Alteration of annealing conditions allows control over grain sizes and the technique can produce large quantities of the desired material.

2.1b *High energy ball mill:*   High energy ball milling is used for the preparation of nanocrystalline alloys. This is sometimes referred to as mechanical alloying or mechanical milling. Nanostructure is obtained by repeated mechanical deformation and alloying as the powder is vigorously shaken in a vial containing a number of milling balls. The energy transfer to the powder particles in these mills takes place by a shearing action or impact of the high velocity balls with the powder. The size of the nanoparticles depends on several factors namely milling speed, type, size, size distribution of balls, ball to powder weight ratio, milling atmosphere etc (McCormink *et al* 1998). This process has the advantage to produce large quantities of material and is already a commercial technology. Contamination from balls should be taken care of.

2.1c *Sputtering:*   This process involves acceleration of ions of elements like argon or krypton to high energies and their bombardment into target materials. Atoms and clusters, both neutral and ionic, are ejected from the target. The ratio of atoms to clusters or ions to neutrals produced depends on the mass and energy of the projectile ion and a variety of other experimental parameters (Stavroyiannis *et al* 1998). For materials with low mutual solubility, co-sputtering is more effective. Contamination problem is less as sputtering is performed under high vacuum. Small cluster formation is a drawback for sputtering. Various sputtering parameters like, environment and its pressure, sputtering power, duration and also annealing of the sputtered film can be used to tune the grain size.
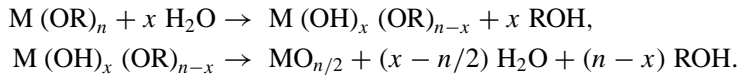
2.1d *Glass-ceramic route:*   Glass-ceramics are produced by controlled crystallization of appropriate glasses. Two-stage heat treatment programs are performed to precipitate various nanocrystalline phases in the parent glass system. The glass specimens are subjected to heat treatment at nucleation and crystallization temperatures respectively. Crystallization temperature is determined form differential thermal analysis (DTA) curve. Nucleation temperature is calculated after knowing the glass transition temperature from DTA curve (Pal *et al* 1997). Nanoparticles remain well protected within the glass matrix.

2.1e *Molecular beam epitaxy:*   This is a technique in which epitaxial layers are grown on a heated substrate by impinging molecular or atomic beams evaporated from effusion sources under ultrahigh vacuum conditions. It differs from conventional evaporative deposition techniques in that the beam intensities of each source and the substrate temperature are separately

controlled to achieve epitaxial growth (Inoue *et al* 1997). MBE has become a very important growth technology not only for semiconductors but also for other material systems like metals, insulators and superconductors. The greatest advantage of this technique is a highly precise control of layer thickness.

2.2 *Chemical methods*

2.2a *Sol–gel route:* Sols are basically dispersions of colloids in liquids. Gelation is the growth and linking together of polymeric units to form a continuous network. This process involves the formation of an (at least in the first step) amorphous network, as distinct from a crystallization process, from solution (Roy 1987). The most widely used starting materials are metal alkoxides. These compounds have the general formula $M(OR)_n$, where M is a metal ion and R is an alkyl group. This process involves formation of an amorphous gel from solution through hydrolysis and polycondensation reactions as follows,

$$M (OR)_n + x\, H_2O \rightarrow M (OH)_x (OR)_{n-x} + x\, ROH,$$
$$M (OH)_x (OR)_{n-x} \rightarrow MO_{n/2} + (x - n/2)\, H_2O + (n - x)\, ROH.$$

Gel product is an amorphous material containing substantial amounts of water and organic residues which can be eliminated by suitable drying treatments. Dehydrated gels are essentially porous materials and further annealing is necessary to produce nanocrystalline materials from these. Low temperature processing is the major advantage of this route. On the other-hand, metal alkoxides are very expensive.

2.2b *Co-precipitation route:* Precipitation of multi component system is known as co-precipitation. This process involves formation of a solid precipitate followed by the separation of the solids with a filtration step. This process needs a co-precipitation agent which can be a solution of inorganic or organic salt. The main condition is that the compound should be insoluble in the mother liquid. Parameters like mixing rate, pH, temperature, concentration etc. have to be properly adjusted (Pathak & Pramanik 2000). Drying and subsequent annealing are required to prepare nanostructured materials by this method.

3. Theoretical background

The fundamental motivation for the preparation and investigation of nanoscale magnetic materials is the dramatic change in magnetic properties in these systems. The magnetic behaviour of most systems is a result of contributions from both interaction and size effects. Magnetic materials consist of a large number of domains within each of which all spins are pointing in the same direction. The domains are separated by domain walls, which have characteristic width and energy associated with their formation and existence. The motion of domain walls contributes to magnetization.

According to the conventional theory for ferromagnetic particles, the temperature dependence of the coercivity H_c in the case of non-interacting particles is given by

$$H_c = H_{c0}[1 - (T/T_B)^{1/2}], \tag{1}$$

where H_{c0} is coercivity at $T = 0$ K.

T_B is the blocking temperature, above which superparamagnetism sets in and is given by

$$T_B = KV/25k, \tag{2}$$

where, K is the anisotropy energy density constant, V the volume of the particle, k the Boltzmann's constant.

The coercivity of fine particles has a marked dependence on their size which is shown in figure 1. As the particle size is reduced, it is found that the coercivity increases, goes through a maximum and then tends towards zero. In the large particle size range, energy considerations favour the formation of domain wall. Magnetization reversal thus occurs through the nucleation and motion of these walls. As the particle size decreases towards some critical diameter, the formation of domain walls becomes energetically unfavourable and the particles form single domains. Changes in the magnetization can no longer occur through domain wall motion and instead require the coherent rotation of spins, resulting in large coercivities. As the particle size continues to decrease below the single domain value, the spins are increasingly affected by thermal fluctuations and the system becomes superparamagnetic.

Many nanostructures exhibit unusual low-temperature behaviour suggestive of that observed in random or disordered magnetic systems. Imry & Ma (1975) showed that random fields, no matter how small, destroy long-range order in most magnetic systems. Randomness produces a range of different types of imperfectly ordered ground states. These states have in common a cusp in the ZFC susceptibility and irreversibility between the ZFC and FC susceptibility. Above blocking temperature (T_B), the particles are free to align with the field during the measuring time and the ZFC curve superimposes with field-cooled (FC) curve. This state is called superparamagnetic, because the particle behaves similarly to paramagnetic spin but with a much larger moment. The experimental criteria for superparamagnetism are (1) the magnetization curve exhibits no hysteresis and (2) the magnetization curves at different temperatures must superpose in a plot of M vs. H/T. Imperfect H/T superposition can result from a broad distribution of particle sizes.

4. Properties

4.1 *Nanocrystalline magnetic alloys*

Among the nanocomposite alloys Fe–Nd–B ternary system has attracted considerable attention as a permanent magnetic material and as recording media. Croat *et al* (1984) have described the hard magnetic properties of melt spun Nd–Fe–B alloys with particle size in the
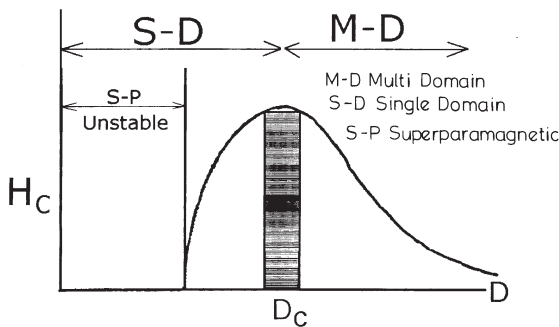

Figure 1. Schematic diagram showing variation of coercivity (H_c) with particle diameter (D) for magnetic material.

range 20–80 nm. They have attained maximum energy product $(BH)_{max} \approx 14 \cdot 1$ MGOe the largest value ever reported for light rare earth iron magnet. They have studied the variation of $(BH)_{max}$ with the substrate surface velocity while maintaing the other parameters fixed. The authors have also investigated the variation of coercivity (H_c) and remanence (B_r) with temperature. They suggest that optimum hard magnetic properties arise due to the formation of single domain particles.

Yang & Roy (1988) have reported $(BH)_{max}$ of 16·6 MGOe for Fe–Nd–B system prepared through melt spun followed by hot extrusion process. They have also reported enhanced M_r values. They proposed that enhanced $(BH)_{max}$ and M_r arise from the formation of a favourable texture.

Magnetic properties of $Nd_2Fe_{14}B(Si)$ melt spun flakes with particle size range 20–100 nm have been reported by Clemente *et al* (1988). They have attained M_r 9·3 kG, M_s 15·7 kG and $(BH)_{max}$ 19MGOe. They proposed that some kind of exchange interaction between the magnetic particles is responsible for high remanence (HIREM). Microanalysis in an analytical electron microscope (AEM) indicates that there are two requirements for HIREM phenomenon to arise, viz. (a) substantial absence of intergranular phase between Nd_2–Fe_{14}–B crystallites, and (b) specific grain size. Silicon addition results in smaller variation in grain size.

A systematic investigation of the influence of melt spinning process conditions on the grain size in the nanocrystalline range and on the magnetic properties of Nd–Fe–B alloys with small silicon additions have been reported by Manaf *et al* (1991). They conclude that the necessary condition for realising remanence enhancement for the alloy system is to reduce the grain size below 30 nm to facilitate magnetic interactions between grains.

After the recognition of exchange-coupled interaction between nanoscale hard and soft magnetic phases, mainly two types of nanocomposites namely, α–Fe/$Nd_2Fe_{14}B$ and $Fe_3B/Nd_2Fe_{14}B$ have been widely studied because of their high M_r and high $(BH)_{max}$ values The motivation for this research has been to combine the advantages of both hard and soft magnetic phases and thereby attain a higher energy product than is otherwise feasible.

Melt spun nanocrystalline exchange coupled Fe–Nd–B magnets with enhanced remanence have been studied by Bauer *et al* (1996). Starting from nearly single phase $Fe_{14}Nd_2B$ magnets, α–Fe has been added in the composite stepwise up to 40 vol% by reducing the Nd and B content. They have achieved maximum M_r 12·5 kOe when α–Fe is 30 vol %, the $(BH)_{max} = 23 \cdot 3$ MGOe whereas the coercive field is 5·3 kOe. From microstructural analysis they find the average particle size to be around 15 and 25 nm corresponding to the α–Fe and $Fe_{14}Nd_2B$ phases respectively.

Magnetic properties of the nanocomposite alloys can be strongly influenced either by incorporating group III or IV elements, such as Si, Ga, Al or by changing the volume fraction of the magnetic phases. Because of its large size La ion has been shown to be an effective glass former when substituted for Nd in Nd–Fe–B alloy system. Chang *et al* (1998) have studied the effect of boron and rare earth contents on the magnetic properties of La and Cr substituted melt spun α–Fe/$R_2Fe_{14}B$ type nanocomposites. It has been found that a slight substitution of Cr for Fe suppresses the formation of $R_2Fe_{23}B_3$ and Fe_3B phases respectively during crystallization and results in the formation of α–Fe/$R_2Fe_{14}B$ mixture. Increasing the total rare earth content is found to enhance the remanence. The authors have attained coercivity around 12 kOe, Br $\approx$ 11·4 kG and $(BH)_{max} \approx$ 19 MGOe.

In order to achieve higher remanence for practical application another two-phase nanocomposite system which has been explored is $Sm_2Fe_{17}N_x/\alpha$–Fe with low Sm content. The trend in this system, which shows single-phase magnetic behaviour, is for the coercivity to rise

as remanence falls, by increasing the proportion of the hard phase. Magnetic properties and microstructure of rapidly quenched Sm–Fe–N powders with low Sm contents and Zr and Co addition have been studied by Yoneyama *et al* (1995). High remanence value of 9·4 kG with a high coercivity of 7–10 kG are obtained for isotropic powder. XRD and TEM studies show that these alloys are composed of Sm–Fe_7N_x and α-Fe phases with sizes in the range 20–30 nm. It is presumed that the high remanence is due to small crystal size and exchange coupling at the interphase boundaries.

Ordinarily Fe–Nd–B system does not have a high glass-forming ability. This is insufficient to obtain nanocomposite permanent magnets in thick melt-spun ribbons. To have good hard magnetic properties in a bulk or thick ribbon Fe–Co–Nd–Dy–B metallic glass system has been explored by Zhang *et al* (2001). They have prepared ribbon thickness upto 250 μm. The crystallized nanocomposite structure consists of $Nd_2Fe_{14}B$, $(Fe, Co)_3B$ and α-(Fe, Co). The remanence B_r and $(BH)_{max}$ values of 12·4 kOe and 13·2 MGOe, respectively, have been attained for the ribbon of 250 μm in thickness annealed at 1176 K for 60 sec.

Ryan *et al* (1997) have investigated the magnetization process in exchange coupled ball milled α-Fe/$Nd_2Fe_{14}B$ nanocomposite by applying Mössbauer spectroscopy. Mössbauer spectra of both components have been extensively studied and excellent fits are available. Measurements confirm that the magnetization of the soft phase is strongly coupled to that of the hard phase and analysis indicates that remanence is dominated by the hard phase.

Effect of grain size of α-Fe on magnetic properties of mechanically alloyed Nd–Fe–B/α-Fe nanocomposite have been investigated by Sun *et al* (1999). The best magnetic properties have been obtained with the average grain size of 15 nm and content of α-Fe around 45 wt % which is well below the structural percolation threshold of the soft magnetic phase. The measured dependence of coercivity on the grain size indicates that the optimum grain size increases with the increase of α-Fe content for $Cm > 30$ wt %. They have explained the size effect on magnetic properties as arising due to the formation of an exchange interaction free zone.

Cui *et al* (2001) have investigated the effect of preparation process on structure and magnetic properties of $Nd_2Fe_{14}B$/α-Fe type nanocomposite magnets. Coercivity, remanence and $(BH)_{max}$ for the system prepared by mechanical milling (MM) are substantially higher than the values of corresponding mechanical alloying (MA) prepared samples. Also the average grain size of both α-Fe and $Nd_2Fe_{14}B$ in the MM prepared samples are measurably smaller than that of the MA prepared samples.

O'Donnell & Coey (1997) have studied a range of exchange coupled two phase mechanically alloyed nanocomposites composed of hard magnetic $Sm_2Fe_{17}N_3$ and soft magnetic α-Fe. TEM studies reveal that grain sizes are in the range 10–50 nm. Addition of Zr and Ta are the most effective in controlling the grain growth during crystallization, reducing the grain size from 20–30 to 10–20 nm. Presence of grain boundary phase between the crystallites has been confirmed by HRTEM. This phase has been confirmed by Mössbauer studies of the samples and has a significant effect on coupling between the two phases.

Effect of pressure on the microstructure and magnetic properties of α-Fe/$Sm_2(Fe, Si)_{17}C_x$ nanocomposite magnets has been studied by Zhang *et al* (2001). The results show that with increasing pressure from normal to 6 GPa, the grain size decreases from 30·6 to 6·4 nm for α-Fe and from 28·7 to 5·8 nm for $Sm_2(Fe,Si)_{17}C_x$. The nanocomposites prepared under 4 GPa have a significant increase in both coercivity and remanent magnetization as compared to those prepared under normal pressure.

To achieve higher density of recording for information storage system Co and Fe based nanocomposite alloys have been explored for the last two decades. These alloys with

equiatomic composition undergo a phase transformation from a disordered face centred cubic (FCC) to an ordered face centred tetragonal (FCT) structure after annealing which has a very high anisotropy. The drive for higher magnetic recording density imposes the need for grain sizes below 10 nm.

DC magnetron sputtered Fe–Pt thin films as a function of Pt content from 0 to 60 at % has been studied by Yung *et al* (1992). Polycrystalline films have been obtained in the range studied. An ordered FCT phase has been found to appear under suitable heat treatment in the sample containing 22 to 50 at % of Pt. For films comprising about 60 at. % Pt, annealing treatment is observed to deteriorate the magnetic properties owing to the formation of an antiferromagnetic phase. Crystalline sizes estimated from TEM analysis are in the range 10 to 60 nm. By suitably annealing the films with about 33 at. % Pt, the authors have obtained a coercivity of 13 kOe.

Magnetic properties of nanocomposite CoPt/Ag films prepared by cosputtering method have been investigated by Stavroyiannis *et al* (1998). As deposited films are found to consist of FCC CoPt which transforms to highly anisotropic FCT phase after annealing at 773 K. The final nanocomposite structure consists of CoPt nanoparticles with the hard FCT structure embedded in an FCC Ag matrix. Large values of coercivity in the range 1–17 kOe have been achieved with grain sizes in the range of 7 to 100 nm.

In order to have high coercivity with low media noise Yu *et al* (1999) have investigated cosputtered CoPt:C nanocomposite films. To form weak exchange coupling between small CoPt grains, C would be ideal isolation material because there exist neither Co nor Pt carbides. Annealing at 873 K gives rise to FCT CoPt nanoparticles with grain sizes of 8–20 nm and coercivities of 3–12 kOe. The properties of these nanocomposite CoPt:C films can be tailored to satisfy the thermal stability, coercivity and media noise requirements for extremely high density recording.

Magnetron sputtered FePt nanocomposite in glassy matrix like B_2O_3 and SiO_2 have been investigated by Luo *et al* (2000). They find that coercivity and particle size highly depend on the annealing temperature and the concentration of the matrix phase. Coercivities in the range 4 to 12 kOe have been obtained for particle sizes in the range 4 to 17 nm.

Zeng & Yan (2001) have investigated the CoPtCr:C nanocomposite films prepared by magnetron sputtering. Magnetic properties such as coercivity and remanence ratio (S) strongly depend upon the Pt and C concentration. Compared with the CoPt:C films, lower exchange coupling and higher S at the same C concentration have been obtained. H_c values ranging from 2 to 10 kOe and S closer to 1 have been achieved for film thicknesses down to 10 nm.

To increase the energy product Liu *et al* (1998) have studied magnetron-sputtered Fe/Pt multilayer system with twice the thickness of iron layer (corresponding roughly to the atomic ratio of Fe:Pt as 2:1). The final nanocomposite films consist of the hard FCT FePt phase and FCC soft magnetic Fe_3Pt phase. The maximum energy products of the optimally processed samples exceed 40 MGOe which is attributed to the exchange interaction between the two phases.

To protect the nanocrystalline magnetic materials researchers have also used some hard matrix like silicon or boron nitride. Maya *et al* (1998) have prepared FeN/CoN nanocomposite films in nitride matrix by using a reactive sputtering technique in a nitrogen plasma. Cobalt nitride decomposes into elements on being heated under vacuum at 773 K and creates a fine dispersion (< 10 nm) of cobalt particles in ceramic matrix. The precursor CoN is paramagnetic while the cobalt particles having dimensions smaller than single magnetic domain, shows superparamagnetism and below blocking temperature, marked hysteresis.

Preparation of hexagonal GaN:Mn and GaN:Fe epilayers by molecular beam epitaxy with very high concentrations of transition metal ions has been reported by Kuwabara *et al* (2001).

Magnetization data show that GaN:Mn epilayers are primarily paramagnetic with ferromagnetic spin exchange represented by the paramagnetic curie temperature around 20 K. The GaN:Fe epilayers exhibit superparamagnetic behaviour which presumably arises from Fe and/or FeN crystallites.

Chatterjee *et al* (1990) have studied the Mössbauer spectra of nanocomposites in the system (Fe–Cr)–SiO_2 prepared by sol gel followed by suitable reduction treatment. The spectra consist of a weak sextet pattern with hyperfine field around 328 kOe attributed to the presence of α–iron. The dominant central doublet with isomersift around 0.29 mm/s and quadrupole splitting around 0.73 mm/s is attributed to nanosized particles of Fe–Cr alloy. The large value of quadrupole splitting arises due to the presence of very fine alloy particles.

Magnetic properties of Fe–Ni nanocrystalline alloys in SiO_2 and Al_2O_3 matrix have been studied by Chien (1991). Coercivity of $(Fe_{50}Ni_{50})_x$ $(Al_2O_3)_{1-x}$ nanocrystalline alloy system changes smoothly as the metal content is increased and drops off sharply at the percolation threshold. Coercivity more than 2 kG was attained at around $x = 50$ vol %. They have observed similar behaviour in the $(Fe_{50}Ni_{50})_x (SiO_2)_{1-x}$ system.

Disorder in chemically prepared nanocrystalline Ni_3Fe particles dispersed in silica matri x has been invstigated by Datta *et al* (1999) by Mössbauer spectroscopy. Ni_3Fe particles with sizes in the range 9·4 to 19·6 nm have been synthesized using sol-gel technique and by changing the concentration of silica and the reducing conditions. Figure 2 shows the Mössbauer spectra of 50 Ni_3Fe–50 SiO_2 nanocomposites. The analysis of Mössbauer spectra shows that the hyperfine field increases as the particle size is reduced. This indicates that the atomic disorder in this alloy increases as the particle size is decreased.

Sabiryanov *et al* (1998) have performed a first principle calculation leading to an energy product of 90 MGOe in a perfect two-phase FePt/Fe nanocomposites. Table 1 summarizes the different metallic alloy systems studied so far and the techniques used for their synthesis.

4.2 *Nanocrystalline magnetic ceramics*

Among magnetic ceramics, ferrites are the only systems which have been explored widely for their behaviour in the nanocrystalline state. As magnetic materials, soft ferrites are best suited for high frequency applications. Hard ferrites are used for making permanent magnets. Nanoparticles of ferrites exhibit magnetic properties markedly different from their
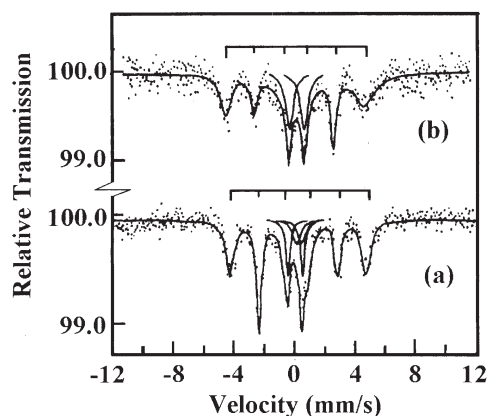

Figure 2. Mössbauer spectra for sample with composition 50 Ni_3Fe–50 SiO_2 and particle size 19·6 nm at **(a)** room temperature, **(b)** 77 K (Pal *et al* 2000).

Table 1. Techniques used for the preparation of various metallic alloy systems and important properties evaluated.

System	Method of preparation	Particle size (nm)	Properties measured	Reference
$Nd_{0.95}(La_{0.05})_{11}$ $Fe_{77}Cr_2B_{10}$	Melt spin	20 / 70	Magnetization (coercivity 13·2 kOe)	Chang *et al* (1998)
NdFeB/α-Fe	Melt spin	40 / 110	Magnetization (BH_{max} 18·8–19·0 MGOe)	Fang *et al* (1997)
$Nd_{12-x}Fe_{(82+x)}$ B_6/α-Fe	Melt spin	20 / 50	Magnetization (BH_{max} 19·0 MGOe)	Chang *et al* (1996)
$(Sm,Zr)Fe_7$ N_x/α-Fe	Melt spin	20·0	Magnetization (remanence 9·9 kG)	Hidaka *et al* (1998)
$Sm_2(Fe, Si)_{17}$ C_x/α-Fe	Melt spin	6·4 / 5·8	Magnetization (effect of pressure)	Zhang *et al* (2001)
Fe–Pt	Sputtering	100	Magnetization (BH_{max} 40·0 MGOe)	Liu & Luo (1998)
CoPt / Ag	Sputtering	7–100	Magnetization (coercivity 1–17 kOe)	Stavroyiannis *et al* (1999)
CoPt : C	Sputtering	8–20	Magnetization (coercivity 3–12 kOe)	Yu *et al* (1999)
(Fe–Cr)–SiO$_2$	Sol–gel	17–83	Mössbauer study (quadrupole splitting around 0·73 mm/s)	Chatterjee *et al* (1990)
SmCox–Co	Sputtering	10·0	Magnetization (coercivity 40 kOe)	Liu *et al* (1999)
Ni$_3$Fe/SiO$_2$	Sol–gel	9·4–19·6	Mössbauer study (hyperfine field 281–292 kOe)	Datta *et al* (1999)

bulk counter parts. For example, Zn–ferrite is a well known normal spinel and exhibit anti-ferromagnetic order below 10 K in bulk form, whereas in nanocrystalline form they show ordering at much higher temperature because of the cation inversion (Chinnasamy *et al* 2001).

Tang *et al* (1991) have reported the behaviour of magnetic transition temperature when the system dimensions are reduced. Nanocrystalline MnFe$_2$O$_4$ particles in the size range 7·5 to 24·4 nm have been prepared by a chemical process. Studies show that Curie temperature (T_c) increases when the particle size is reduced and goes to nanoscale range. When particle size is 7·5 nm, T_c is 97 K higher than that for the bulk material. The shift in curie temperature can be rationalised by the finite size-scaling formula with proper exponent and amplitude.

Studies on ultrafine and nearly spherical Mn–Zn ferrite particles prepared by the hydrothermal process have been reported by Pannaparyil & Komarneni (1991). Average particle size obtained is about 11·5 nm. The particle size distribution of these fine crystallites has been estimated from the hyperfine field distribution. Superparamagnetic behaviour has been observed in the case of particles having dimensions less than 10 nm. It is also reported that hydrothermal ferrite powders could be sintered to almost theoretical densities at relatively low temperatures.

Nanocrystalline barium ferrite particles in the size range 5–100 nm have been synthesized by thermal decomposition of a citrate precursor. The precursor decomposed at 700 K is amorphous and crystallization of the nanocrystalline ferrite phase starts from a temperature 700 K. The ferrite shows a monophase X-ray diffraction pattern and well, resolved Mössbauer spectra are obtained at 973 K. Mössbauer spectra at both liquid helium and room temperature of samples annealed at different temperatures could be satisfactorily resolved into fine ferrite by Sankarnarayan *et al* (1993).

Pal *et al* (1997) have reported the preparation and charactarization of nanocrystalline barium hexaferrite particles dispersed in a borate glass matrix. Particles in the size range 8·2 to 17·6 nm have been grown by a suitable two-stage heatreatment. Low temperature magnetization measurements have been carried out. Variation of coercivity as a function of temperature for different samples are shown in figure 3. Coercivity is found to be much smaller than the bulk ferrite. Also it is found that coercivity increases when the temperature is lowered or the particle size is increased. The authors have attributed this behaviour to a change in the value of effective anisotropy constant as the particle size is varied.

Low temperature magnetization studies have been performed by Koutani & Gavoille. (1994) on *rf* sputtered nanocrystalline Co-ferrite particles. Average particle size obtained is about 8 nm. They report low magnetization compared with that of the bulk. Results indicate that the long range ferromagnetic order is broken in the films and glassy behaviour takes over.

Hamdeh & Ho (1997) have reported the preparation by aerogel procedure of Zn–ferrite with an average particle size 10 nm and inversion parameter of 0·21. X-ray, magnetization, Mössbauer and calorimetry studies have been carried out. The magnetic states of the as-prepared and annealed samples are best described as disordered which depend on temperature. The grain sizes have been varied over a wide range by ball milling and also the inversion parameter can be changed to 0·55 by such procedure.

Nanocrystalline $MnFe_2O_4$ particle with diameters in the range 13·7 to 100 mn have been synthesized through conventional ceramic route in the system $x Nb_2O_5 (50-x) MnO \, 50Fe_2O_3$ where $0 < x < 20$, by Kundu & Chakravorty (1999). It was proposed that Nb^{5+} ions give rise to vacancies in the Mn^{2+} sites, which break up the coupling of ferrimagnetically active oxygen polyhedra. The decrease of Curie temperature with $MnFe_2O_4$ particle size been explained on the basis of a decrease in the number of exchange pairs of the type Mn^{2+} and Fe^{3+}. It has
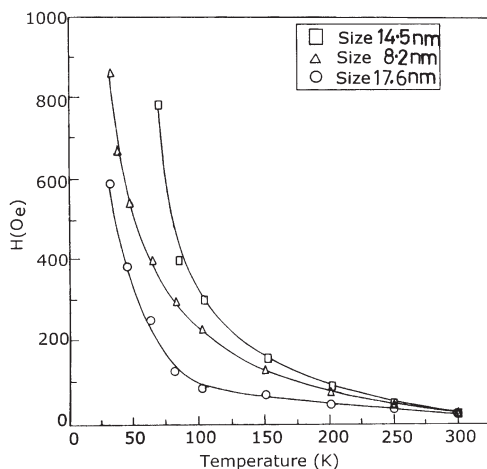

Figure 3. Variation of coercivity (H_c) as a function of temperature (T) for different nanocrystalline barium hexaferrite samples (Pal *et al* 1997).
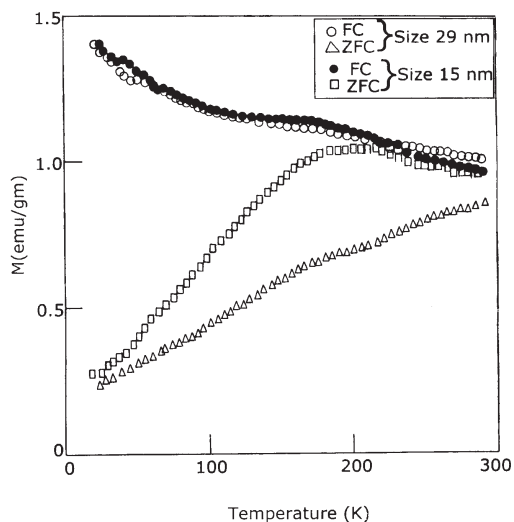
Figure 4. Magnetization vs. temperature plots measured at field-cooled (FC) and zero field-cooled (ZFC) condition for nanocrystalline Ni–Zn ferrite (Pal *et al* 1996).

been observed that coercivity increases and saturation magnetization decreases as the size of $MnFeO_4$ is reduced.

Effect of grain size on cation distributions, magnetic properties and type of ordering in nanocrystalline ball milled $CdFe_2O_4$ has been reported by Chinnasamy *et al* (2001). Sizes of the prepared samples are in the range 7–77 nm. The magnetization measurements reveal a spin glass like surface structure and material is found to have a large anisotropy. The cation inversion is found to increase with the decrease in particle size.

Magnetic properties at low temperature for nanocrystalline Ni–Zn ferrite in a borate glass matrix prepared by the glass ceramic route have been reported by Pal *et al* (1996). Nanocrystals in the size range 15–29 nm have been grown by a two stage heat treatment in the temperature range 873–953 K. Maximum coercivity estimated for 0 K (H_{c0}) is about 334 Oe when the corresponding ferrite particle size is 15 nm. Figure 4 delineates the magnetization vs. temperature curve measured both in FC and ZFC conditions. FC and ZFC magnetization data for different samples are consistent with the blocking temperature extracted from variation of coercive force with temperature. Higher anisotropy is attributed to the small particle size.

Nanocomposites consisting of nanometer sized nickel zinc ferrite and α–iron have been prepared by subjecting micrometer sized ferrite particles to a reduction treatment by Pal *et al* (2000). The materials have been characterized by XRD, TEM, Mössbauer spectroscopy and magnetization measurements. By controlling the reduction schedule a wide range of magnetic moments and coercivity can be obtained. It appears that reduction process breaks down the particle size of precursor nickel zinc ferrite powder thereby giving rise to nanocrystalline particles. Table 2 summarizes the various nanocrystalline ferrite systems studied so far and the preparation techniques used for their synthesis.

5. Summary

We have reviewed the different physical and chemical techniques exploited for growing nanocrystals of magnetic phases either metallic or ceramic. The coercivity in these materials can be changed drastically by varying the particle size or the matrix in which they

Table 2. Techniques used for the preparation of nanocrystalline ferrite systems.

System	Method of preparation	Particle size (nm)	Properties measured	Reference
$BaFe_{12-2x}Ti_x$ Co_xO_{19}	Glass-ceramic	100–200	Magnetization	Kubo *et al* (1985)
$ZnFe_2O_4$	Coprecipitation	2–6	Mössbauer (low temperature)	Sato *et al* (1990)
Mn–Zn ferrite	Hydrothermal	11·5	Mössbauer Magnetization	Pannaparayil & Komarneni (1991)
Ni–Zn ferrite	Chemical route	15–19	Magnetization (coercivity 250 Oe)	Pal *et al* (1996)
$CoFe_2O_4$	Sol–gel	10–76	Magnetization (coercivity 5400 Oe)	Kim *et al* (2001)
Ba–hexaferrite	Glass-ceramic	8·2–17·6	Magnetization	Pal *et al* (1997)
α-Fe/Fe$_3$O$_4$	Conventional ceramic	20 / 80	Magnetization (magnetic moment 96 emu/gm)	Tokumitsu & Nasu (2001)
Mn–ferrite	Conventional ceramic	13·7–100	Magnetization	Kundu & Chakravorty (1999)
α-Fe$_x$ $(BaFe_{12}O_{19})_{1-x}$	Ball mill	10·0	Magnetization (magnetic moment 150 emu/gm)	Gonzalez *et al* (2000)
α-Fe/Ni–Zn ferrite	Sol–gel	15–20	Mössbauer study	Pal *et al* (2000)

are dispersed. The highest value of energy product $(BH)_{max}$ in the case of melt spun Nd–Fe–B alloys have been reported for particle size around 20 nm. A much larger value of 40 MGOe has however been reported for multiplayer Fe/Pt system containing hard magnetic phase FePt and soft magnetic phase Fe$_3$Pt respectively. Cobalt and iron based nanocomposite alloys exhibit coercivity as high as 17 kOe for grain sizes of the order of 100 nm. Mössbauer studies reveal disorder in Ni$_3$Fe alloys dispersed in silica matrix with particle size of 9·4 nm. Nanocrystalline soft ferrites e.g., MnFe$_2$O$_4$, (Ni$_{0·5}$Zn$_{0·5}$)Fe$_2$O$_4$ show an increase of coercivity as compared to of their bulk counterparts. The Curie temperature appears to depend markedly on their particle size in these systems. Nanocomposites of α–iron and (Ni$_{0·5}$Zn$_{0·5}$)Fe$_2$O$_4$ show a wide range of magnetization and coercivity depending on the volume fractions of the components present.

References

Bauer J, Seeger M, Zern A, Kronmuller H 1996 Nanocrystalline FeNdB permanent magnets with enhanced remanence. *J. Appl. Phys.* 80: 1667–1673

Chang W C, Hsing D M 1996 Magnetic properties and transmission electron microscopy microstructures of exchange coupled $Nd_{12-x}Fe_{82+x}B_6$ melt spun ribbons. *J. Appl. Phys.* 79: 4843–4845

Chang W C, Chiou D Y, Wu S H 1998 High performance α-Fe/$Nd_2Fe_{14}B$ type nanocomposites. *Appl. Phys. Lett.* 72: 121–123

Chang W C, Chiou D Y, Wu S H 1998 The effect of boron and rare earth contents on the magnetic properties of La and Cr substituted α-Fe/$R_2Fe_{14}B$ type nanocomposites. *J. Appl. Phys.* 83: 6271–6273

Chatterjee A, Das D, Chakravorty D, Choudhury K 1990 Mössbauer spectra of nanocrystalline Fe and Fe–Cr particles in sol–gel derived SiO_2, glass. *Appl. Phys. Lett.* 57: 1360–1362

Chien C L 1991 *Science & technology of nanostructured magnetic materials* (eds) G C Hadjipanayis, G A Prinz (New York: Plenum)

Chinnasamy C N, Narayansamy A, Ponpandian N, Chattopadhyay K, Guerault H, Greneche J -M 2001 Ferrimagnetic ordering in nanostructured zinc ferrite. *Scr. Mater.* 44: 1407–1410

Chinnasamy C N, Narayansamy A, Ponpandian N, Joseyphus R J, Chattopadhyay K, Shinoda K, Jeyadevan B, Tohji K, Nakatsuka K, Guerault H, Greneche J-M 2001 Structure and magnetic properties of nanocrystalline ferromagnetic $CdFe_2O_4$ spinel. *Scr. Mater.* 44: 1411–1415

Chudnovsky E M, Gunther L 1988 Quantum tunneling of magnetization in small ferromagnetic particles. *Phys. Rev. Lett.* 60: 661–664

Clemente G B, Keem J E, Bradley J P 1988 The microstructure and compositional influence upon HIREM behaviour in $Nd_2Fe_{14}B$. *J. Appl. Phys.* 64: 5299–5301

Croat J J, Herbst J F, Lee R W, Pinkerton F E 1984 Pr-Fe and Nd-Fe-based materials: A new class of high-performance permanent magnets. *J. Appl. Phys.* 55: 2078–2082

Cui B Z, Sun X K, Xiong L Y, Liu W, Zhang Z D, Yang Z Q, Wang A M 2001 Effect of preparation process on structure and magnetic properties of $Nd_2Fe_{14}B$/α-Fe type nanocomposite magnets. *J. Mater. Res.* 16: 709–715

Datta A, Pal M, Chakravorty D, Das D, Chintalapudi S N 1999 Disorder in nanocrystalline Ni_3Fe. *J. Magn. Magn. Mater.* 205: 301–306

Dormann J L, Fiorani D 1992 *Magnetic properties of fine particles* (Amsterdam: North-Holland)

Fang J -S, Hsieh M -F, Chen S -K, Chin T -S 1997 Magnetic properties and structure of Nd (Fe,B) nanocomposite alloys with fixed Fe/B ratio at 4–14. *Jap. J. Appl. Phys.* 36: 6316–6324

Gonzalez J, Montero M I, Crespo P, Marin P, Hernando 2000 Hysteresis and relaxation of hard–soft nanocomposite samples. *J. Appl. Phys.* 87: 4759–4761

Hamdeh H H, Ho J C 1997 Magnetic properties of partially inverted zinc ferrite aerogel powders. *J. Appl. Phys.* 81: 1851–1857

Hidaka T, Yamamoto T, Nakamura H, Fukuno A 1998 High remanence (Sm, Zr)$Fe_7N_x + \alpha$-Fe nanocomposite magnets through exchange coupling. *J. Appl. Phys.* 83: 6917–6919

Imry Y, Ma S-K 1975 Random-field instability of the order state of continuous symmetry. *Phys. Rev. Lett.* 35: 1399–1401

Inoue N, Kawamura Y, Morimoto K 1997 Molecular beam epitaxy. *Handbook of nanophase materials* (ed.) A N Goldstien (New York: Marcel Dekker) pp 83–140

Kim W C, Lee C W, Kim C S 2001 Magnetic properties of Co-Bi ferrite powders and thin films by a sol-gel method. *Scr. Mater.* 44: 1451–1455

Kittel C 1946 Theory of the structure of ferromagnetic domains in films and small particles. *Phys. Rev.* 70: 965–971

Knella E F, Luborsky F E 1963 Particle size dependency of coercivity and remanence of single domain particles. *J. Appl. Phys.* 34: 656–658

Kodama R H, Berkowitz A E, McNiff E J, Jr Foner S 1996 Surface spin disorder in $NiFe_2O_4$ nanoparticles. *Phys. Rev. Lett.* 77: 394–397

Koutani S, Gavoille G 1994 Magnetic behaviour of nanocrystalline cobalt ferrite films. *J. Magn. Magn. Mater.* 138: 237–243

Kubo O, Ido T, Yokohama H, Koike Y 1985 Particle size effects on magnetic properties of $BaFe12-2x$ Ti_xCo_xO19 fine particles. *J. Appl. Phys.* 57: 4280–4282

Kundu T, Chakravorty D 1999 Nanocrystalline $MnFe_2O_4$ produced by niobium doping. *J. Mater. Res.* 14: 3957–3961

Kuwabara S, Ishii K, Haneda S, Kondo T, Munekata H 2001 Preparation of wurtzite GaN based magnetic alloy semiconductors by molecular beam epitaxy. *Physica* E10: 224–228

Liu J P, Liu Y, Skomski R, Sellmyer D J 1999 Magnetic hardening in $SmCo_x$–Co multilayers and nanocomposites. *J. Appl. Phys.* 85: 4812–4814

Liu J P, Luo C P, Liu Y, Sellmyer D J 1998 High energy product in rapidly annealed nanoscale Fe/Pt multilayers. *Appl. Phys. Lett.* 72: 483–485

Luo C P, Liou S H, Gao L 2000 Nanostructured $FePt:B_2O_3$ thin films with perpendicular magnetic anisotropy. *Appl. Phys. Lett* 77: 2225–2227

Manaf A, Buckley R A, Davies H A, Leonowiez M 1991 Enhanced magnetic properties in rapidly solidified Nd-Fe-B based alloys. *J. Magn. Magn. Mater.* 101: 360–362

Mantinez B, Obradors X, Balcells Ll, Rouanet A, Monty C 1998 Low temperature surface spin-glass transition in γ-Fe_2O_3 nanoparticles. *Phys. Rev. Lett.* 80: 181–183

Maya L, Thompson J R, Song K J, Warmack R J 1998 Thermal conversion of an iron nitride-silicon nitride precursor into a ferromagnetic nanocomposites. *J. Chem. Phys.* 83: 905–910

McCormick P G, Miao W F, Smith P A I, Ding J, Street R 1998 Mechanically alloyed nanocomposite magnets. *J. Appl. Phys.* 83: 6256–6261

O'Donnell K, Coey J M D 1997 Characterization of hard magnetic two-phase mechanically alloyed $Sm_2Fe_{17}N_3/\alpha$-Fe nanocomposites. *J. Appl. Phys.* 81: 6310–6321

Pal M, Brahma P, Chakravorty D, Bhattacharyya D, Maiti H S 1997 Preparation of nanocrystalline barium hexaferrite in a glass medium. *Nanostruct. Mater.* 8: 731–738

Pal M, Brahma P, Chakravorty D, Bhattacharyya D, Maiti H S 1996 *J. Magn. Magn. Mater.* 164: 256–260

Pal M, Das D, Chintalapudi S N, Chakravorty D 2000 Preparation of nanocomposites containing iron and nickel-zinc ferrite. *J. Mater. Res.* 15: 683–688

Pannaparayil T, Komarneni S 1991 Hyperfine fields and particle size distribution in small particles Mn–Zn ferrites. *Phys. Status Solidi* A126: 443–450

Pardos C, Multigner M, Hernando A, Sanchez J C, Fernandez A, Conde C F, Conde A 1999 Dependence of exchange anisotropy and coercivity on the Fe-oxide structure in oxygen-passivated Fe-nanoparticles. *J. Appl. Phys.* 85: 6118–6120

Parker F T, Spada F F, Cox T J, Berkowitz A E 1996 Mössbauer effect study of metal particle tape stability. *J. Magn. Magn. Mater.* 162: 122–130

Parkin S S, More N, Roche K P 1990 Oscillations in exchange coupling and magnetoresistance in metallic superlattice structures: Co/Ru, Co/Cr and Fe/Co. *Phys. Rev. Lett.* 64: 2304–2307

Pathak A, Paramanik P 2000 *Nanoparticles of oxides through chemical route (Nanomaterials)* (ed.) D Chakravorty D pp. 47–70

Ping D H, Hono K 1998 Partitioning of Ga and Co atoms in a Fe3B / Nd2Fe14B nanocomposite magnet. *J. Appl. Phys.* 83: 7769–7775

Roy R 1987 Ceramics by the solution-sol-gel route. *Science* 238: 1664–1669

Ryan D H, Feutrill E H, Ding J 1997 Magnetization process in a two phase exchange coupled system: A microscopic study. *J. Appl. Phys.* 81: 4425–4427

Sabiryanov R F, Jaswal S S 1998 Electronic structure and magnetic properties of hard/soft multilayers. *J. Magn. Magn. Mater.* 177–181 989

Sankarnarayan V K, Pankhurst Q A, Dickson D P E, Johnson C E 1993 An investigation of particle size effects in ultrafine barium ferrite. *J. Magn. Magn. Mater.* 125: 199–208

Sato T, Haneda K, Seki M, Iijima T 1990 Morphology and magnetic properties of ultrafine ZnFe2O4 particles. *Appl. Phys.* A50: 13–16

Stavroyiannis S, Panagiotopoulos I, Niarchos D 1998 CoPt/Ag nanocomposites for high density recording media. *Appl. Phys. Lett.* 73: 3453–3455

Stavroyiannis S, Panagiotopoulos I, Niarchos D 1999 New CoPt/Ag nanocomposites for high density recording media. *J. Appl. Phys.* 85: 4304–4306

Sun X K, Zhang J, Chu Y, Liu W, Cui B, Zhang Z 1999 Dependence of magnetic properties on grain size of α-Fe in nanocomposite $(Nd,Dy)(Fe,Co,Nd,B)_{5.5}/\alpha$-Fe magnets. *Appl. Phys. Lett.* 74: 1740–1742

Tang Z X, Sorensen C M, Klabunnde K J 1991 Size-dependent curie temperature in nanoscale $MnFe_2O_4$ perticles. *Phys. Rev. Lett.* 67: 3602–3605

Tokumitsu K, Nasu T 2001 Preparation of lamellar structured α-Fe/Fe_3O_4 complex particle by thermal decomposition of wustite. *Scr. Mater.* 44: 1421–1424

Yang C J, Roy R 1988 Development of texture in extruded Fe–Nd–B magnets. *J. Appl. Phys.* 64: 5296–5298

Yoneyama T, Yamamoto T, Hidaka T 1995 Magnetic properties of rapidly quenched high remanence Zr added Sm–Fe–N isotropic powders. *Appl. Phys. Lett.* 67: 3197–3199

Yu M, Liu Y, Moser A, Weller D, Sellmyer D J 1999 Nanocomposite CoPt:C films for extremely high-density recording. *Appl. Phys. Lett.* 75: 3992–3994

Yung S W, Chang Y H, Lin T J, Hung M P 1992 Magnetic properties and microstructure of iron–platinum thin films. *J. Magn. Magn. Mater.* 116: 411–418

Zeng H, Yan M L 2001 CoPtCr:C nanocomposite films for high density recording. *J. Appl. Phys.* 89: 810–812

Zhang D, Klabunde K J, Sorensen C M, Hadijipanayis G C 1998 Magnetization temperature dependence in iron nanoparticles. *Phys. Rev.* B58: 14167–14170

Zhang W, Inoue A 2001 Influence of ribbon thickness on the formation and magnetic properties of melt spun Fe–Co–Nd–B metallic glasses. *J. Appl. Phys.* 89: 1509–1511

Zhang X Y, Zhang J W, Wang W K 2001 Effect of pressure on the microstructure of α-Fe/$Sm_2(Fe,Si)_{17}C_x$ nanocomposite magnets. *J. Appl. Phys.* 89: 477–481